

Orphan nuclear receptor NR4A1 regulates both osteoblastogenesis and adipogenesis in human mesenchymal stem cells

YILAN JIN^{1,2}, YOUNGHO SON³, INSUN SONG^{1,2}, YOON-SOK CHUNG^{1,2} and YONG JUN CHOI^{1,2}

¹Department of Endocrinology and Metabolism, Ajou University School of Medicine, Suwon, Gyeonggi-do 16499, Republic of Korea;

²Ajou Institute on Aging, Ajou University Medical Center, Suwon, Gyeonggi-do 16499, Republic of Korea;

³Department of Physiology, Ajou University School of Medicine, Suwon, Gyeonggi-do 16499, Republic of Korea

Received January 16, 2024; Accepted September 19, 2024

DOI: 10.3892/mmr.2024.13368

Abstract. The nuclear receptor subfamily 4 group A member 1 (*NR4A1*) gene plays a crucial role in both osteoporosis and adipogenesis. The present study investigated the mechanisms by which *NR4A1* influences osteoblastogenesis and adipogenesis in human bone marrow-derived mesenchymal stem cells (BMD-MSCs). *NR4A1* was overexpressed or knocked down in mouse MC3T3-E1 osteoblast cells and 3T3-L1 adipocyte cells, as well as in PCS-500-012, a BMD-MSC line. The alkaline phosphatase (ALP) assay and Alizarin Red S staining were performed using MC3T3-E1 and BMD-MSCs to assess ALP activity and mineralization, while Oil Red O staining was used to assess the lipid content in 3T3-L1 cells and BMD-MSCs. Total RNA was isolated from control, *NR4A1*-overexpressing and *NR4A1* small interfering RNA (siRNA; *siNR4A1*)-treated BMD-MSCs. RNA sequencing (RNA-seq) was performed to identify differentially expressed genes, followed by ingenuity pathway analysis (IPA) to determine the role of *NR4A1* in osteoblastogenesis and adipogenesis. *NR4A1* or *Nr4a1* knockdown tended to increase ALP activity and significantly increased calcification in BMD-MSCs ($P < 0.005$) and MC3T3-E1 cells ($P < 0.005$), respectively. By contrast, *NR4A1* or *Nr4a1* overexpression significantly decreased ALP activity and calcification. *NR4A1* or *Nr4a1* knockdown and overexpression significantly decreased and increased adipogenesis, respectively, in BMD-MSCs ($P < 0.005$ and < 0.05 , respectively) and 3T3-L1 cells ($P < 0.005$ in both). Treatments of BMD-MSCs with an *NR4A1* antagonist, 1,1-bis(3'-indolyl)-1-(p-hydroxyphenyl) methane and *siNR4A1* showed similar results. RNA-seq and IPA in control, *NR4A1* knockdown and *NR4A1* overexpressing cells indicated that Notch signaling mediated the effects of

NR4A1 in osteoblastogenesis and adipogenesis. Expression of mastermind-like transcriptional coactivator 3 was reduced in the Notch signaling pathway in cells treated with *siNR4A1*. In conclusion, *NR4A1* suppressed osteoblastogenesis and promotes adipogenesis in human BMD-MSCs. The present study also suggested that *NR4A1* plays a role in the progression of osteoporosis and adipogenesis by modulating the Notch signaling cascade.

Introduction

The global prevalence of obesity and osteoporosis is growing with the increase in the life expectancy and number of aged individuals. Mesenchymal stem cells (MSCs) are the common progenitor of both adipocytes and osteoblasts and delicately balance their differentiation processes (1). An elevated shift in commitment of MSCs toward adipogenesis increases the adipocyte population (2,3), which may lead to osteoporosis. Studies have shown that the number of adipocytes in the bone marrow increases with aging, and individuals with a heightened adipocyte count in their bone marrow typically exhibit declined bone density (4-6).

In our previous study, next-generation RNA sequencing (RNA-seq) of bone marrow MSCs identified differentially expressed genes (DEGs) between patients with osteoporosis and postmenopausal women with normal bone mineral density. Ingenuity Pathway Analysis (IPA) of these DEGs identified *NR4A1*, encoding nuclear receptor subfamily 4A member 1, as a key gene associated with osteoporosis and adipocyte differentiation (7).

The *NR4A* subfamily genes encode proteins that regulate various cellular processes such as cell cycle, apoptosis, steroidogenesis, adipogenesis and energy metabolism (8-10). The expression levels of these genes have been shown to be elevated in extreme obesity but return to normal following fat reduction, suggesting their association with obesity (8). Additionally, the parathyroid hormone induces the expression of *NR4A* family proteins in bone (11-13). A previous study has shown an interaction between *NR4A* receptors and the β -catenin signaling pathway in osteoblasts, where *NR4A* receptors inhibit β -catenin-mediated transactivation, crucial for bone tissue formation and function (14), suggesting a potential role of *NR4A* family proteins in bone metabolism.

Correspondence to: Professor Yong Jun Choi, Department of Endocrinology and Metabolism, Ajou University School of Medicine, 164 Worldcup, Yeongtong, Suwon, Gyeonggi-do 16499, Republic of Korea
E-mail: colsmile@hanmail.net

Key words: adipogenesis, mesenchymal stem cell, *NR4A1*, orphan nuclear receptor, osteoblastogenesis

However, the precise role of the NR4A family proteins in MSCs remains to be elucidated.

The present study aimed to investigate the effects of modulation of *NR4A1* expression on differentiation of MSCs into osteoblasts and adipocytes. Furthermore, using IPA, it sought to clarify the common pathways and related genes involved in the regulation of *NR4A1*-mediated regulation of MSC differentiation.

Materials and methods

Cell culture. Mouse MC3T3-E1 pre-osteoblast cells (CRL-2593; ATCC) were cultured in Minimum Essential Medium supplemented with 10% fetal bovine serum (Gibco; Thermo Fisher Scientific, Inc.) and 1% antibiotic-antimycotic (Gibco; Thermo Fisher Scientific, Inc.). Mouse fibroblast cell line 3T3-L1 (CL-173; ATCC) was cultured in the high glucose Dulbecco's Modified Eagle's Medium supplemented with 10% fetal bovine serum and 1% antibiotic-antimycotic (Gibco; Thermo Fisher Scientific, Inc.). BMD-MSCs (passage 2; cat. no. PCS-500-012; ATCC; expressing CD29, CD44, CD73, CD90, CD105, and CD166 markers; not expressing CD14, CD19, CD31, CD34, and CD45 markers) were maintained in the basal medium (cat. no. PCS-500-030; ATCC) supplemented with growth factors (cat. no. PCS-500-041; ATCC). All cells were plated following small interfering RNA (siRNA) or clone transfection. MC3T3-E1 cells and BMD-MSCs were plated at a density of 1.0×10^4 cells/well in 48-well plates and used for osteoblast differentiation. After 24 h of culturing in the plates, the cells were stimulated with an osteogenic medium containing ascorbic acid (50 $\mu\text{g}/\text{ml}$; cat. no. 50-81-7; MilliporeSigma) and β -glycerophosphate (10 mM; cat. no. 13408-09-8; MilliporeSigma) for cell adherence (day 0) and cultured for 18 days. The cells were subjected to alkaline phosphatase (ALP) assay on days 3, 5 and 7 and Alizarin Red S (ARS) staining on days 7, 14 and 18. 3T3-L1 cells and BMD-MSCs were seeded at a density of 5.0×10^4 cells/well in 30 mm plates, stimulated with the adipogenic medium containing 1 μM dexamethasone (cat. no. 50-02-2; MilliporeSigma), 0.5 mM isobutylmethylxanthine (cat. no. 28822-58-4; MilliporeSigma), 10 μM insulin (cat. no. 11061-68-0; MilliporeSigma) and 200 μM indomethacin (cat. no. 53-86-1; MilliporeSigma) for differentiation into adipocytes and cultured for 9 and 18 days, respectively. To investigate NR4A1 expression levels, the 3T3-L1 cells were subjected to a 9-day incubation period, while the BMD-MSCs were incubated for 20 days. Throughout the incubation process, the culture medium was replaced every 3 days. All cells were incubated at 37°C in a humidified environment with 95% air and 5% CO₂.

Plasmids, lentivirus packaging and reagents. Full-length mouse *Nr4a1*wt (cat. no. BC004770; pCMV-SPORT6-Nr4a1), human *NR4A1*wt (cat. no. NM_002135; pCMV-SPORT6-NR4A1), and the pCMV-SPORT6 plasmid (Mock) were provided by the Korea Human Gene Bank (Medical Genomics Research center, KRIBB, Korea). All cells were cultured at a density of $\sim 1 \times 10^5$ /well in 6-well plates, and plasmids were transfected with 100 pmol/ml siRNA using Lipofectamine® 2000 (cat. no. 11668019; Invitrogen; Thermo Fisher Scientific, Inc.) in Opti-MEM (Gibco; Thermo Fisher Scientific, Inc.) at 37°C

for 48 h. Small interfering RNAs (siRNAs) for mouse *Nr4a1* (*siNr4a1*, 5'-GCAAGCCUACCAUGGACCU-3', 5'-AGGUCC AUGGUAGGCUUGC-3'), human *NR4A1* (*siNR4A1*, 5'-GUG AAGGAAGUUGUCCGA A-3', 5'-UUCGGACAACU CCUUCAC-3') and NC-siRNA (Negative control siRNA; cat. no. SN-1002) were obtained from Bioneer Corporation. Control and *NR4A1*-overexpressing BMD-MSCs were plated at a density of 4.0×10^5 cells per well in 100 mm plates and treated with 20 μM 1,1-bis(3'-indolyl)-1-(p-hydroxyphenyl) methane (DIM-C-pPhOH; cat. no. HY-112055; MedChemExpress), an NR4A1 antagonist (15), and incubated at 37°C for 24 h before being subjected to osteoblast or adipocyte differentiation.

Reverse transcription-quantitative (RT-q) PCR. RT-qPCR was performed to determine *NR4A1* mRNA expression levels, and its expression was normalized with those of mouse or human *Actb* (cat. no. NM_007393)/*ACTB* (cat. no. NM_001101; both Bioneer Corporation) mRNA, serving as internal standards. Cells were cultured at a density of $\sim 1 \times 10^5$ /well in 6-well plates, and transfected with plasmid or siRNA. Total RNA was isolated from cultured cells 48 h after transfection with siRNA or plasmids using TRIzol® (Thermo Fisher Scientific, Inc.) according to the manufacturer's instructions, and its quality was assessed using a spectrophotometer (Beckman Coulter, Inc.). Following extraction, RNA was reverse-transcribed for 1 h at 42°C using a premix kit containing oligo-dT as a primer (iNTRON Biotechnology). The ABI Prism 7000 Sequence Detection System (Applied Biosystems; Thermo Fisher Scientific, Inc.) was used for all PCR measurements. All PCR was performed in triplicate with cycling conditions as follows: Initial denaturation at 95°C /10 min; (ii) 40 cycles of 95°C/30 sec, 60°C/1 min; and 72°C/30 sec using the SYBR Green I qPCR kit (Takara Bio, Inc.) in a total volume of 25 μl , containing 150 ng cDNA according to the manufacturer's guidelines. Gene expression levels were quantified relative to that of *Actb/ACTB* mRNA using the manufacturer-recommended comparative threshold method (Applied Biosystems). The values are expressed as fold-change from the control levels. The relative gene expression was expressed as $2^{-\Delta\Delta C_q}$. The fold-change was determined to be $2^{-\Delta\Delta C_q}$ (16). The primers used for PCR are listed in Table I.

Western blotting. Cells, 48 h after transfection with siRNA or plasmids, were lysed using 0.1 M NaCl, 0.01 M Tris-HCl (pH 7.6), 1 mM ethylenediaminetetraacetic acid (pH 8.0), 1 mg/ml aprotinin, and 100 mg/ml phenylmethylsulfonyl fluoride. Protein concentrations in cell lysates were measured using the Bio-Rad protein assay. Subsequently, 50 μg protein was denatured at 95°C for 5 min in sodium dodecyl sulfate sample buffer, electrophoresed on 10% sodium dodecyl sulfate-polyacrylamide gels, and transferred to polyvinylidene difluoride membranes. The membranes were blocked in 5% skim milk for 1 h at 20–22°C, then incubated overnight at 4°C with primary antibodies against NR4A1 (cat. no. MA5-32647, 1:500; Thermo Fisher Scientific, Inc.) or β -Actin (cat. no. A300-491A, 1:10,000; Bethyl Laboratories, Inc.). Subsequently, the membranes were incubated at 20–22°C for 60 min with an anti-rabbit secondary antibody (1:5,000; Santa Cruz Biotechnology, Inc.). Protein bands were detected using an ECF western blotting kit (Amersham Biosciences; Cytiva)

Table I. Primers for real-time polymerase chain reaction.

Gene	Accession no.	Forward primer sequence (5'→3')	Reverse primer sequence (5'→3')
<i>hACTB</i>	NM_001101	GATGAGATTGGCATGGCTTT	CACCTTCACCGTTCCAGTTT
<i>hNR4A1</i>	NM_001202233	AGAAGATCCCTGGCTTTGCT	CAGGGACATCGACAAGCAAG
<i>mActb</i>	NM_007393	GATCTGGCACCACACCTTCT	GGGGTGTGAAGGTCTCAA
<i>mNr4a1</i>	NM_001411253	GACTTGCTCTCTGGTTCCCT	AGAAGGCCAGGATGTTGTCA
<i>hMAML3</i>	NM_018717	CGTATATCCAGCAGCAGCAA	TTTCTGGTCTTCGCTCAGGT
<i>hJAG1</i>	NM_000214	AAGGGGTGCGGTATATTTC	TCCCGTGAAGCCTTTGTAC
<i>hDTX4</i>	NM_001300727	ACCCAGACTGCAAACCATC	CCGGAAGGTAACAGTGTTCG
<i>hNOTCH3</i>	NM_000435	CTCATCCGAAACCGCTCTAC	TCTTCCACCATGCCCTCTAC
<i>hHES1</i>	NM_005524	TCAACACGACACCGGATAAA	TCAGCTGGCTCAGACTTTCA
<i>hPSEN2</i>	NM_000447	GTGCCTGTCACTCTGTGCAT	GCGTGTAGATGAGCTGTCCA

ACTB, β -actin; NR4A1, nuclear receptor subfamily 4 group A member 1; MAML3, mastermind like transcriptional coactivator 3; JAG1, jagged canonical Notch ligand 1; DTX4, deltex E3 ubiquitin ligase 4; NOTCH3, notch receptor 3; HES1, notch receptor 3; PSEN2, presenilin 2.

and visualized using an Automatic X-RAY Film Processor (cat. no. JP-33; JPI Healthcare Co., Ltd.). Adobe Photoshop 2024 (Adobe Systems, Inc.) was used for densitometry.

ALP and ARS staining. ALP staining was performed on days 3, 5, and 7, and ARS staining was performed on days 7, 14 and 18 in control, *siNr4a1* (or *siNR4A1*)-treated, and *Nr4a1* (or *NR4A1*)-overexpressing MC3T3-E1 cells and human BMD-MSCs. Briefly, for ALP staining, cultured cells were fixed in 10% formalin for 10 min, permeabilized in 0.1% Triton X-100 in phosphate-buffered saline (PBS) for 30 min, and treated for 10–30 min with nitro blue tetrazolium and 5-bromo-4-chloro-3-indolyl phosphate at 20–22°C. Subsequently, 200 μ l extraction solution was added to the samples and incubated at 4°C overnight to determine calcium deposition in the extracellular matrix. Total cell lysates were homogenized in a solution containing 1 mM Tris-HCl (pH 8.8), 0.5 percent Triton X-100, 10 mM MgCl₂, and 5 mM p-nitrophenyl phosphate at 20–22°C. The absorbance at 405 nm was then determined (BioTek Instruments, Inc.).

For ARS staining, cultured cells were fixed in 70% ethyl alcohol for 1 h at 20–22°C. After washing with 1XPBS, the cells were incubated for 10 min at 20–22°C with a 40 mM ARS solution (pH 4.2; cat. no. A5533, MilliporeSigma) to stain the calcium deposits. Prior to staining, the medium was discarded and rinsed gently with 1XPBS. The cells were then extracted with 10% (w/v) cetylpyridinium chloride in 10 mM sodium phosphate to determine the degree of mineralization at pH 7.0. The concentration was determined by measuring the absorbance at 562 nm using a multi-plate reader (cat. no. 1681135; Bio-Rad Laboratories, Inc.) and a standard curve obtained using ARS in the same solution. Each value was expressed as a fold-change compared with control.

Oil Red O staining. Cells were fixed in 10% formalin and stained for 15 min at room temperature according to the manufacturer's instructions using a Lipid (Oil Red O) Staining Kit (cat. no. MAK194; MilliporeSigma). After staining, the cells were washed with double distilled water and four fields

were selected randomly for observation under a fluorescence microscope at 20X or 40X magnification using bright-field illumination (Axiovert 200FL; Carl Zeiss AG). Oil Red O dye was extracted with 100% isopropyl alcohol, and the absorbance was measured at 520 nm using a spectrophotometer (SpectraMax iD3; Molecular Devices, LLC) to quantify the lipid content.

mRNA sequencing. Total RNA was quantified using a NanoDrop8000 spectrophotometer (Thermo Fisher Scientific Inc.), and RNA quality was determined using a 2100 Expert Bioanalyzer (Agilent Technologies, Inc.) and an RNA 6000 Nano Kit (Agilent Technologies, Inc.). mRNA libraries for high-throughput transcriptome sequencing were then prepared using Illumina technology (Illumina Inc.).

Preprocessing, expression and functional analysis. The raw sequencing data was trimmed using Cutadapt (v.2.3; github.com/marcelm/cutadapt/releases/tag/v2.3) to eliminate adapters and low-quality reads (Phred score 20) following a previous study (17). Subsequently, the high-quality reads were mapped to the reference genome (hg38) using STAR (v.2.7.0f; Alexander Dobin, Cold Spring Harbor Laboratory; github.com/alexdobin/STAR/tree/2.7.0f) (18), and gene counts were quantified using quantMode option. The DEGs were determined using DESeq2 (v.1.22.1; Bioconductor; anaconda.org/bioconda/bioconductor-deseq2/files?page=2&sort=ndownloads&sort_order=asc&type=&version=1.22.1) software, which employs negative binomial distribution models to analyze the raw count data. Enrichment analysis of DEGs was performed using IPA (QIAGEN Inc.; qiagenbioinformatics.com/products/ingenuity-pathway-analysis) with the Core Analysis feature to identify Canonical Pathways. Pathways with a z-score absolute value of ≥ 2 and a $P < 0.05$ were considered to indicate a statistically significant difference.

Statistical analysis. The statistical analysis was conducted using one-way ANOVA followed by Tukey's post-hoc comparisons. $P < 0.05$ was considered to indicate a

statistically significant difference. The results were expressed as the mean \pm standard error of the mean (SEM; * $P < 0.05$, ** $P < 0.005$).

Results

NR4A1 mediates the calcification of pre-osteoblast cells and BMD-MSCs. In MC3T3-E1 cells and human BMD-MSCs, *Nr4a1* and *NR4A1*, respectively, were successfully knocked down and overexpressed (Fig. 1A, B and C, G and H, and Fig. S1). *Nr4a1* or *NR4A1* knockdown tended to enhance ALP activity while it significantly increased mineralization in both MC3T3-E1 cells and BMD-MSCs ($P < 0.005$), respectively compared with those in control cells. By contrast, both ALP activity and mineralization were significantly reduced in the respective *Nr4a1* (*NR4A1*) overexpressing groups [MC3T3-E1 cells ($P < 0.05$, $P < 0.005$) and BMD-MSCs ($P < 0.005$; Fig. 1D-F, I-K; showing results of ALP and ARS staining on days 7 and 18 of culture, Fig. S2A and B; showing results of ALP on days 3, 5, and 7, and ARS staining on days 7, 14, and 18, respectively]. These findings suggested that NR4A1 plays a negative role in osteoblast differentiation.

NR4A1 is associated with adipocyte differentiation. To determine whether NR4A1 plays a role in adipogenesis, *Nr4a1* or *NR4A1* overexpression and knockdown were performed in 3T3-L1 cells and BMD-MSCs, respectively (Fig. 2A, B and C and Fig. 1G and H and Fig. S1). Adipogenesis was significantly increased following *Nr4a1* and *NR4A1* overexpression in 3T3-L1 cells ($P < 0.005$) and BMD-MSCs, respectively ($P < 0.05$) compared with those in control cells. By contrast, knockdown of *Nr4a1* and *NR4A1* led to significantly decreased adipogenesis in 3T3-L1 cells ($P < 0.005$ vs. control; Fig. 2D and F) and BMD-MSCs ($P < 0.005$ vs. control; Fig. 2E and G), respectively. These findings indicated that NR4A1 served a beneficial role in adipogenesis.

NR4A1 antagonist modulates osteogenesis and adipogenesis in BMD-MSCs. Subsequently, control and *NR4A1*-overexpressing BMD-MSCs were treated with DIM-C-pPhOH to confirm the effect of NR4A1 on osteogenesis and adipogenesis. The ALP assay was performed on days 3, 5 and 7, while ARS staining was performed on days 7, 14 and 18 of culture. ALP activities tended to increase in both normal and *NR4A1*-overexpressing BMD-MSCs treated with DIM-C-pPhOH compared with those in untreated normal control cells (Fig. 3A-D, Fig. S2C; showing results of ALP on days 3, 5 and 7, and ARS staining on days 7, 14 and 18, respectively). Additionally, adipocyte differentiation was significantly enhanced in the *NR4A1*-overexpressing group compared with that in the control group ($P < 0.005$; Fig. 3E and F). By contrast, DIM-C-pPhOH treatment in both normal and *NR4A1*-overexpressing groups significantly reduced adipocyte differentiation compared with those in their respective untreated control groups ($P < 0.005$). These results indicated that the effects of the treatment with DIM-C-pPhOH were comparable to those of *NR4A1* knockdown in normal cells (Fig. 3E and F). Together, these findings suggested that NR4A1 downregulated osteoblastogenesis but promoted adipogenesis.

NR4A1 effect is related to the Notch signaling pathway. To evaluate the mechanism by which NR4A1 modulated osteoblastogenesis and adipogenesis, DEGs were identified in BMD-MSCs in which *NR4A1* was either knocked down or overexpressed. IPA revealed the association between the changes in *NR4A1* expression and Notch signaling in osteoblastogenesis and adipogenesis. In particular, IPA demonstrated that cells treated with *siNR4A1* had reduced expression of the Mastermind-like transcriptional coactivator 3 (*MAML3*) and elevated expression levels of Jagged canonical Notch ligand 1 (*JAG1*), Deltex E3 ubiquitin ligase 4 (*DTX4*), Notch receptor 3 (*NOTCH3*), Hes family bHLH transcription factor 1 (*HES1*), and Presenilin 2 (*PSEN2*). RT-qPCR data indicated similar results for *MAML3* in *NR4A1* overexpressing ($P < 0.05$) and *NR4A1* knocked down ($P < 0.005$) cells (Fig. 4A and B). Additionally, manipulating the expression of *NR4A1* did not significantly affect expression levels of *NR4A2* or *NR4A3* (Fig. S3).

Discussion

The NR4A subfamily of nuclear receptors serves an important role in various cellular processes. Expression levels of members of the NR4A subfamily of nuclear receptors have been shown to be upregulated in human obesity (8). Furthermore, in 3T3-L1 adipocytes, insulin and insulin sensitizers, such as thiazolidinediones, have been shown to induce the expression of both Nur77 (NR4A1) and Nor-1 (NR4A3), suggesting their potential involvement in adipogenesis (19). The present study investigated whether and how *NR4A1* regulated osteoblast and adipocyte differentiation of BMD-MSCs.

Numerous studies have reported a relationship between *Nr4a1* expression and adipogenesis; however, their findings are not consistent. For instance, Nagai *et al.* (20) demonstrate an indirect association between *Nr4a1* and adipogenesis. Based on this study, estrogen enhances the expression of NR4A1 in muscle cells, leading to an increase in ATP and mitochondrial DNA. Their work suggests an indirect association between adipogenesis and overall energy metabolism in muscle cells rather than directly proving the significance of NR4A1 in adipocyte differentiation. The present study specifically examined adipocyte precursor cells and presented direct evidence of the involvement of NR4A1 in the process of adipocyte development. Qin *et al.* (21) report that permanently increased NR4A1 expression reduces adipogenesis in 3T3-L1 cells and that *Nr4a1* knockdown mice are prone to obesity, suggesting the association between NR4A1 and dysregulation of adipocyte differentiation. Moreover, several *Nr4a1*-responsive genes, such as gap-junction protein 1 and toll-like 1, have been shown to generally suppress adipocyte differentiation (22,23). The present study, for the first time to the best of the authors' knowledge, examined the effects of *NR4A1* on cell fate in stem cells and demonstrated the crucial role of *NR4A1* in enhancing adipocyte differentiation in MSCs. However, the adipogenesis-promoting effect of *Nr4a1* in BMD-MSCs was found to be less pronounced than in 3T3-L1, which may be due to different regulatory networks or additional factors specific to BMD-MSCs. Furthermore, the observations of the present study indicated a marginal increase in *Nr4a1* (NR4A1) expression in *siNr4a1* (*siNR4A1*)-treated cells and a decrease

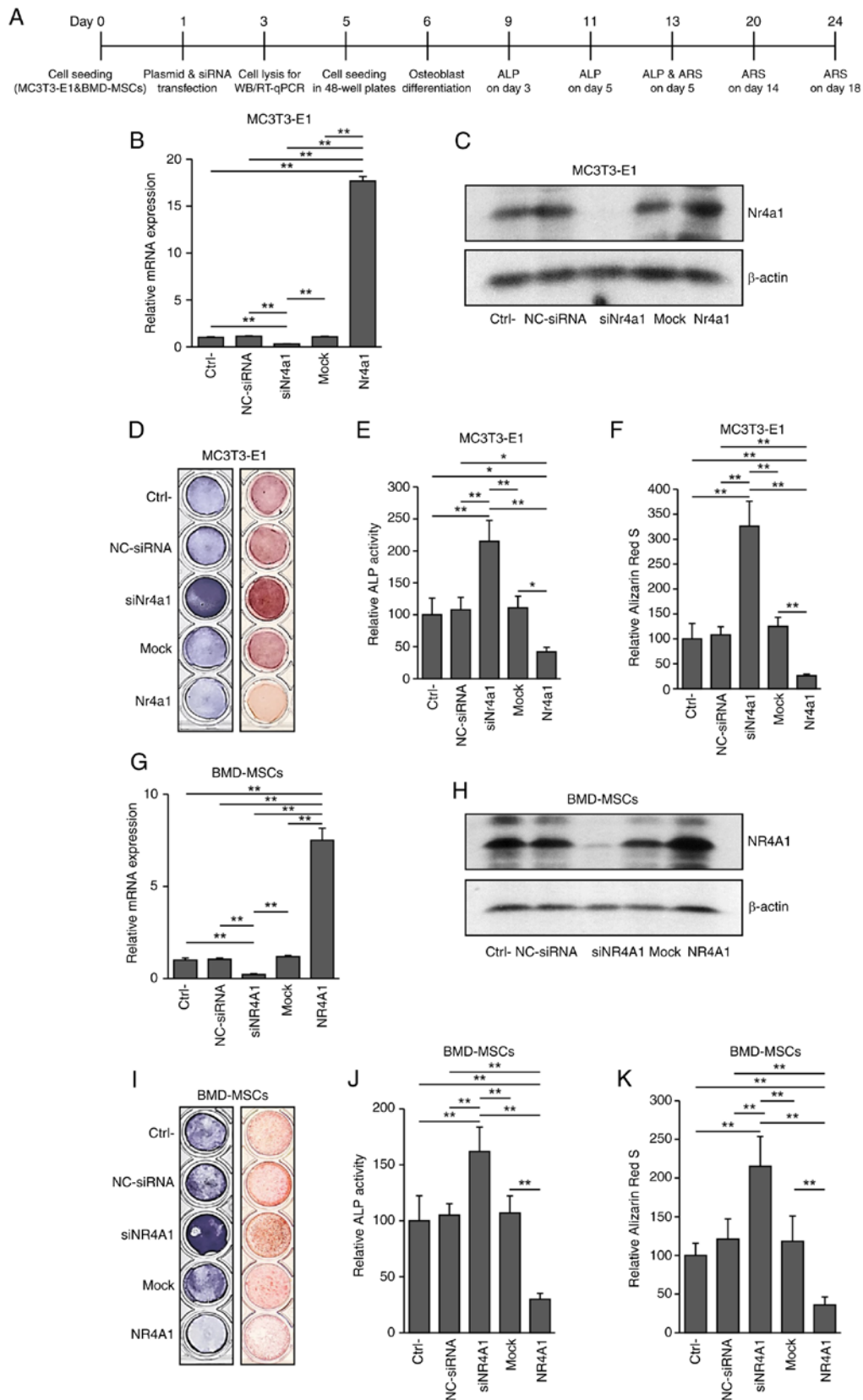


Figure 1. Effects of *Nr4a1* or *NR4A1* knockdown or overexpression in MC3T3-E1 cells and human BMD-MSCs. (A) Experimental design diagram. (B) Reverse transcription-quantitative PCR of *Nr4a1* (*NR4A1*) and (G) mRNA expression in MC3T3-E1 cells and BMD-MSCs. (C and H) Western blot analysis of NR4A1 expression in MC3T3-E1 cells and BMD-MSCs. (D) ALP staining performed on day 5 and (I) Alizarin red S staining performed on day 18 of culture. (E and J) ALP activity measured at 405 nm using alkaline phosphatase yellow liquid substrate system. (F and K) Alizarin red S-stained cells were extracted using cetylpyridinium chloride, and the mineralization level was quantified by measuring absorbance at 562 nm in control, *siNr4a1* (*siNR4A1*)-treated, and *Nr4a1* (*NR4A1*)-overexpressing cells. Data are presented as the mean \pm standard errors of the mean of three biological replicates. *P<0.05, **P<0.005 vs. control. NR4A1, nuclear receptor subfamily 4 group A member 1; BMD-MSCs, bone marrow-derived mesenchymal stem cells; ALP, alkaline phosphatase; Ctrl-, Control; NC, negative control; si, small interfering; *siNr4a1*, *siNr4a1*-treated MC3T3-E1 cells; *siNR4A1*, *siNR4A1*-treated BMD-MSCs; *Nr4a1*, *Nr4a1*-overexpressing MC3T3-E1 cells; *NR4A1*, *NR4A1*-overexpressing BMD-MSCs.

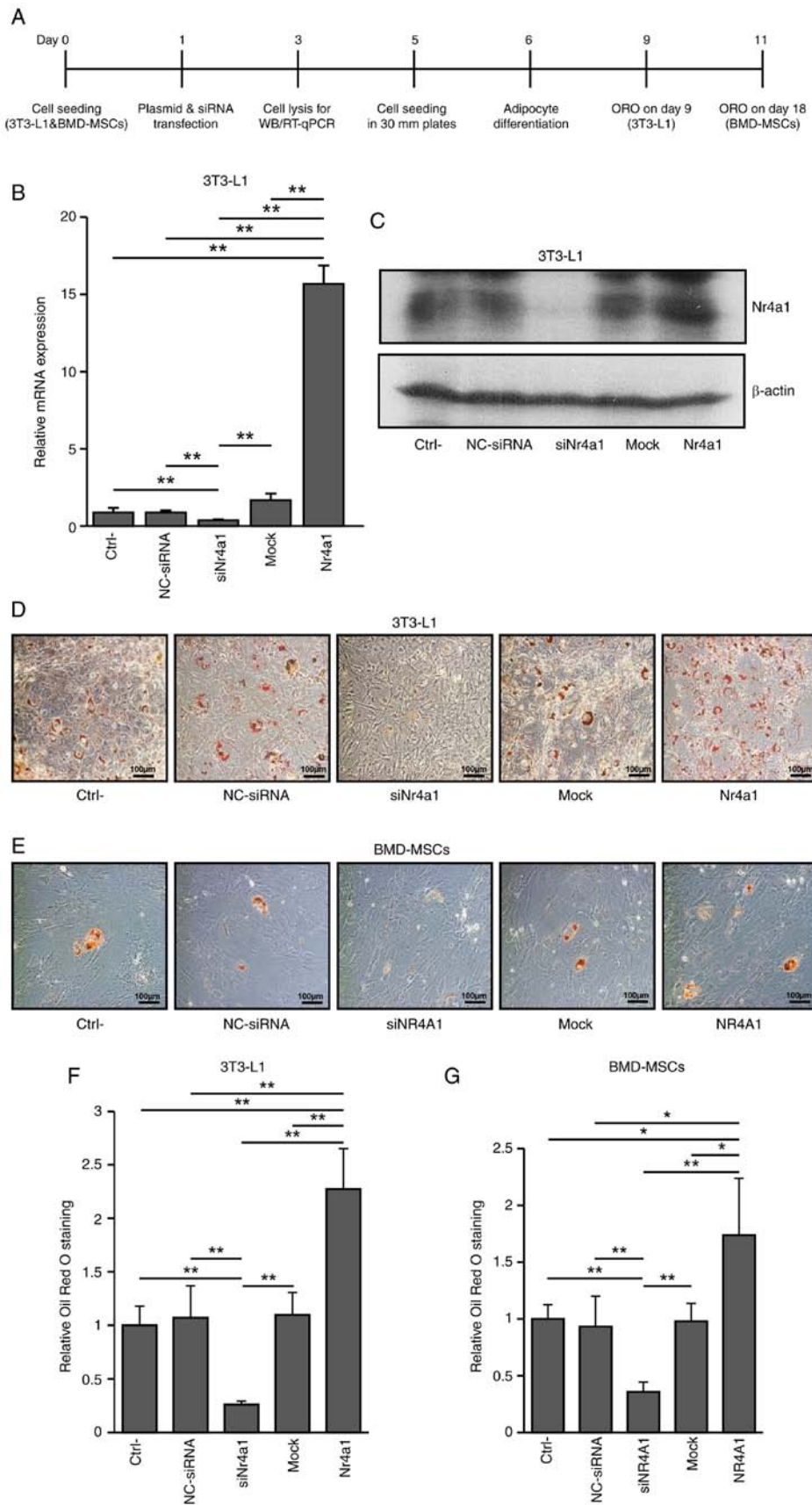


Figure 2. *Nr4a1* (*NR4A1*)-overexpression increases adipogenesis in 3T3-L1 cells and BMD-MSCs. (A) Experimental design diagram. (B) Reverse transcription-quantitative PCR of *Nr4a1* mRNA expression in 3T3-L1 cells. (C) Western blot analysis of NR4A1 expression in 3T3-L1 cells. (D) Adipocyte differentiation and (F) quantification of *Oil Red O* staining in control, *siNr4a1* (*siNR4A1*)-treated and *Nr4a1* (*NR4A1*)-overexpressing 3T3-L1 cells. (E) Adipocyte differentiation and (G) quantification of *Oil red O* staining in control, *siNr4a1* (*siNR4A1*)-treated, and *Nr4a1* (*NR4A1*)-overexpressing BMD-MSCs. Data are presented as the mean \pm standard errors of the mean of three biological replicates. * $P < 0.05$, ** $P < 0.005$ vs. control. NR4A1, nuclear receptor subfamily 4 group A member 1; BMD-MSCs, bone marrow-derived mesenchymal stem cells; Ctrl-, Control; NC, negative control; si, small interfering; *NR4A1* *NR4A1*-overexpressing BMD-MSCs.

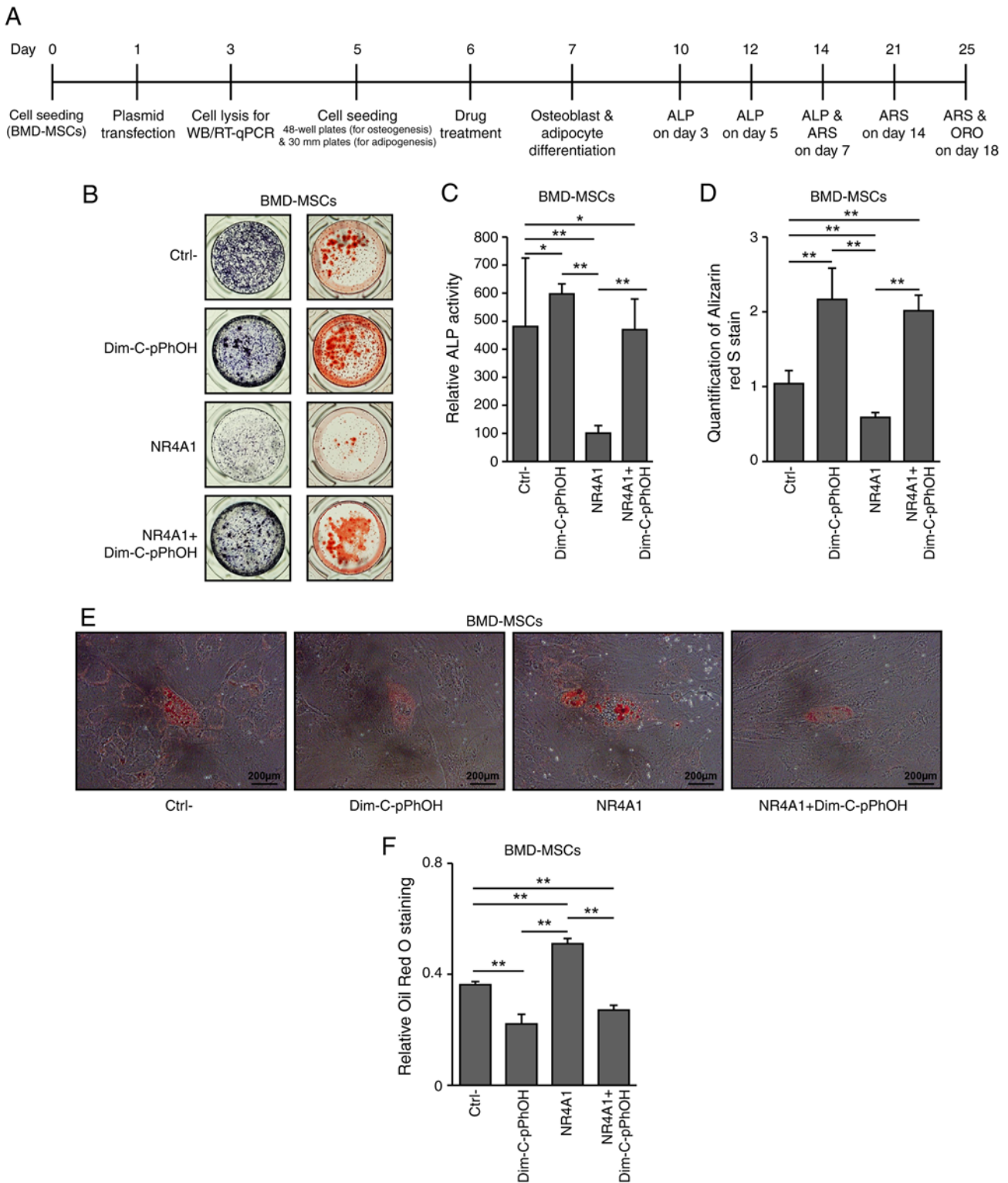


Figure 3. DIM-C-pPhOH and *NR4A1* knockdown demonstrate similar effects on adipogenesis in BMD-MSCs. (A) Experimental design diagram. (B) ALP staining and Alizarin red S staining were performed on days 7 and 18 of culture, respectively. (C) ALP activity measured at 405 nm using alkaline phosphatase yellow liquid substrate system. (D) Alizarin red S-stained cells were extracted using cetylpyridinium chloride, and the mineralization level was quantified by measuring absorbance at 562 nm in control, DIM-C-pPhOH-treated, *NR4A1*-overexpressing, and *NR4A1*-overexpressing/DIM-C-pPhOH-treated BMD-MSCs. (E) Adipocyte differentiation and (F) quantification of Oil red O staining in human BMD-MSCs. * $P < 0.05$, ** $P < 0.005$. DIM-C-pPhOH, 1,1-bis(3'-indolyl)-1-(p-hydroxyphenyl) methane; NR4A1, nuclear receptor subfamily 4 group A member 1; BMD-MSCs, bone marrow-derived mesenchymal stem cells; ALP, alkaline phosphatase; Ctrl-, Control; NC, negative control; si, small interfering; *NR4A1* *NR4A1*-overexpressing BMD-MSCs.

in Nr4a1 (NR4A1) overexpressing cells over time (Fig. S4). These fluctuations in expression levels are commonly seen in transient transfection and would not have been detectable

with permanent transfection. The relatively reduced effect in BMD-MSCs cells can be ascribed, to some extent, to the transient nature of our transfection method. This transient

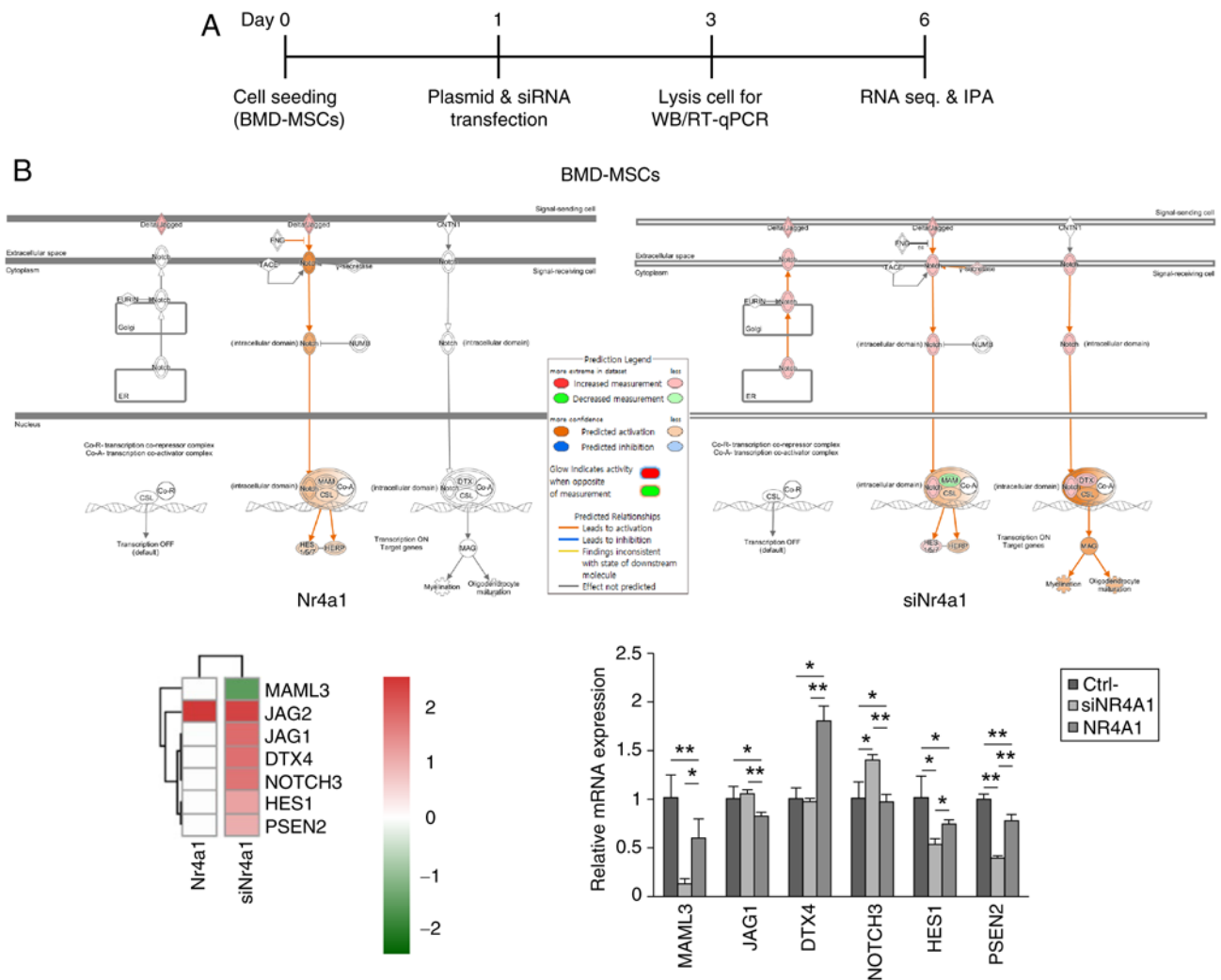


Figure 4. Notch signaling mediates the effects of NR4A1 on osteoblastogenesis and adipogenesis in BMD-MSCs. (A) Experimental design diagram. (B) IPA revealed that the expression of the gene encoding the Notch signaling pathway component MAML3 was decreased, whereas those of *JAG1*, *DTX4*, *NOTCH3*, *HES1* and *PSEN2* were increased in *siNR4A1*-treated cells. RT-qPCR data of the representative genes showing altered expression in IPA. Similar changes were observed in *MAML3* mRNA expression. Data are presented as the mean \pm standard errors of the mean of three biological replicates. * $P < 0.05$, ** $P < 0.005$. NR4A1, nuclear receptor subfamily 4 group A member 1; BMD-MSCs, bone marrow-derived mesenchymal stem cells; IPA, ingenuity pathway analysis; MAML3, Mastermind-like transcriptional coactivator 3; RT-qPCR, reverse transcription-quantitative PCR; WB, western blot analysis; Ctrl-, Control; si, small interfering; *siNr4a1*, *siNr4a1*-treated MC3T3-E1 cells; *siNR4A1*, *siNR4A1*-treated BMD-MSCs; *Nr4a1*, *Nr4a1*-overexpressing MC3T3-E1 cells.

transfection probably had its main effect during the initial stages of adipogenesis, which may have limited its long-term influence on the overall differentiation process. Methodological variations and gene expression mechanisms may account for the differences observed in the present study compared with those of Qin *et al.* (21) and Chao *et al.* (22). While the aforementioned studies used stable cell lines infected with lentivirus for permanent transfection, the present study employed transient transfection, which can cause fluctuations in NR4A1 expression. This transient expression may lead to varying effects on adipogenesis, particularly in the early stages, but may not fully reflect long-term effects. Additionally, NR4A1 interactions with other factors could influence adipogenesis differently. Qin *et al.* (21) noted that increased GATA2 and p53 expression might inhibit adipogenesis, while Chao *et al.* (22) found that Nur77, Nurr1 and Nor1, including NR4A1, generally suppress adipocyte differentiation. By contrast, the present study showed that NR4A1 promoted adipocyte differentiation, possibly due to different regulatory networks or other factors specific to

MSCs. The marginal fluctuations in NR4A1 expression in the present study, owing to the transient transfection method, could further explain the divergence in findings compared with studies using permanent transfection. The experiments of the present study employed transient transfection to manipulate NR4A1 expression, a methodological choice for capturing the dynamic nature of adipogenesis and calcification processes. Permanent transfection was not considered because it has the potential to obscure dynamic changes, compromise cell viability, and introduce artifacts by continuously driving gene expression, which may not accurately reflect natural cellular regulation (24). Instead, transient transfection was chosen to capture the temporal dynamics crucial for the analysis and more effectively ensure the integrity of our research process.

It is worth noting that a previous study demonstrated that siRNA constitutive expression of Nur77 (Nr4a1) prevents adipogenesis, whereas its transient overexpression increases adipogenesis in NIH-3T3 cells (25). That study also shows that Nur77 siRNA and constitutive expression delay adipogenesis

in 3T3-L1 cells, accompanied by prolonged mitotic clonal expansion (25). It also suggests that Nur77 promotes adipocyte differentiation by clonal expansion during the initial phases of adipocyte development and the regulation of the progression of the cell cycle (25). Based on the previous research and the present study, it can be inferred that NR4A1 plays a role in directing MSCs toward adipocytes in the stem cell phase and promoting transient clonal expansion in the early preadipocyte stage. Many complex regulatory mechanisms are involved in the adipogenesis process. For instance, the RNA-seq analysis of the present study revealed that fatty acid binding protein 4 (*FABP4*) expression increased in *NR4A1* overexpressing cells, while it was decreased in *siNR4A1*-treated cells. By contrast, the expression of other key adipogenesis-related genes, including CCAAT/enhancer binding proteins (*CEBPs*) and peroxisome proliferator-activated receptor gamma (*PPARγ*), did not alter (Fig. S5). However, changes in the expression of these genes did not qualify for differential expression analysis, suggesting *NR4A1* influences adipogenesis through some distinct mechanisms. Therefore, further studies are required to elucidate the precise role and function of *NR4A1* in this intricate process.

Fewer studies have explored the potential role of NR4A1 in osteoblast differentiation compared with the number of studies on its role in adipocyte differentiation. NR4A1 has been suggested to be a critical regulator of osteoclast biology and bone remodeling, making this nuclear receptor an attractive target for osteoporosis therapy (26). Parathyroid hormone injection has been shown to rapidly and transiently enhance the expression of all NR4A family members in target tissues *in vivo* and NUR77 activated by PTH influences osteoblast development by increasing cAMP-PKA signaling (12,27). Although the role of NR4A1 in bone formation is not fully understood, these studies indicate that NR4A1 may affect osteoblastogenesis. In the present study, calcification was increased in human BMD-MSCs with *NR4A1* knock-down, whereas it was decreased in *NR4A1*-overexpressing BMD-MSCs. These findings suggested that NR4A1 negatively regulates osteoblastogenesis in MSCs.

DIM-C-pPhOH binds to NR4A1 and acts as an antagonist, inhibiting NR4A1-dependent transactivation and showing antineoplastic activity. DIM-C-pPhOH causes changes in gene expression comparable to those of *NR4A1* knockdown by RNAi (15,28-30). For instance, treatment with DIM-C-pPhOH suppresses NR4A1 overexpression and cancer cell proliferation and promotes apoptosis in breast, pancreatic and lung cancers (15,28,31). Similarly, when BMD-MSCs were treated with DIM-C-pPhOH, anticipating an antagonistic effect on NR4A1, identical outcomes were observed in the cells treated with DIM-C-pPhOH and *siNR4A1*. These findings confirmed that NR4A1 had a negative effect on osteoblastogenesis, whereas it apparently stimulated adipogenesis in BMD-MSCs. Together, these data suggested that DIM-C-pPhOH could be a new therapeutic agent targeting both osteoporosis and obesity. Nevertheless, further research is needed to confirm this hypothesis.

The present study examined the effects of *NR4A1* up- and downregulation of genes in BMD-MSCs. The IPA analysis indicated the presence of multiple interconnected pathways such as Notch signaling, Sonic Hedgehog Signaling, Gas Signaling and Gαq Signaling (Data not shown). Of all the

pathways, the Notch pathway exhibited contrasting effects on adipogenesis and osteoblastogenesis, which aligned with the present study. Notch signaling has been speculated to interact with Wingless-type MMTV integration site family or bone morphogenetic protein pathways directly or indirectly in osteoblasts, osteocytes, and osteoclasts, regulating skeletal tissue development (32). The commitment of MSCs to the osteoblastic lineage is inhibited by Notch1, which suppresses the transactivation activity of Runt-related transcription factor 2 (*Runx2*) (33) and Notch2 inactivation, specifically in osteoblasts (*Notch2fl/fl/Runx2-Cre*), leads to increased trabecular bone formation and enhances osteogenic capacity, underscoring Notch2 as a key inhibitor of osteoblast differentiation (34). Mesenchymal progenitor cell proliferation and differentiation are controlled by Notch signaling, which is dependent on the recombination signal binding protein-J (35). When expressed in immature osteoblasts, Notch inhibits their development, resulting in osteopenia. By contrast, Notch expression in osteocytes initially inhibits bone resorption and increases bone volume in mice (36). Notch also regulates the expression of transcription factors triggered by fatty acids and is essential for adipogenesis (37). Notch decreases the levels of Hes-1, which is necessary for the initial phase of adipogenesis (38). Notch signaling increases osteogenic differentiation but inhibits adipogenesis in primary human MSCs (39). Taken together, Notch signaling inhibits adipogenesis by decreasing the expression of adipogenic transcription factors such as *PPARγ* and *C/EBPα*, particularly through the activation of Notch1 and *Jagged1* (38,39). In the present study, IPA showed that *MAML3* expression was significantly reduced in *NR4A1*-knocked down BMD-MSCs. Furthermore, RT-qPCR findings showed most similar patterns of alterations in the expression of *MAML3* and other genes related to Notch signaling. *MAML3* is a member of the Notch signaling pathway, which is conserved throughout metazoans and essential for cell proliferation, differentiation and death (40). Human *MAML3* stabilizes the DNA-binding complex of RBP-J/CBF-1 protein and the Notch intracellular domains, which act as signaling intermediates (41). RBP represses coactivation by NF-κB and another cellular transcription factor, *C/EBP-b* (42). These observations are consistent with the literature and the present study, where Notch signaling promotes bone-forming cells (osteoblasts) but inhibits fat cell formation (adipocytes). This dual functionality underscores the significant role of Notch in determining cell fate within the MSC population.

In a previous study, *NR4A1* was suggested to be important for osteoporosis and adipogenesis (7). The present study found that osteoblastogenesis was increased in the *NR4A1* knockdown group and decreased in the *NR4A1* overexpression group. Significantly increased adipogenesis was observed in the *NR4A1* overexpression group, whereas decreased adipogenesis was observed in the *NR4A1* knockdown group. Thus, the anticipated functions of NR4A1 in human BMD-MSCs were confirmed in our experiments. According to the RNA-seq and IPA that compared gene expression in control, *siNR4A1*-treated, and NR4A1 overexpressing cells, Notch signaling was expected to be the common pathway of NR4A1, related to both osteoblastogenesis and adipogenesis. Numerous studies have linked Notch signaling to osteogenesis or adipogenesis in stem cells (33,35). In this study, analysis of the expression of associated Notch

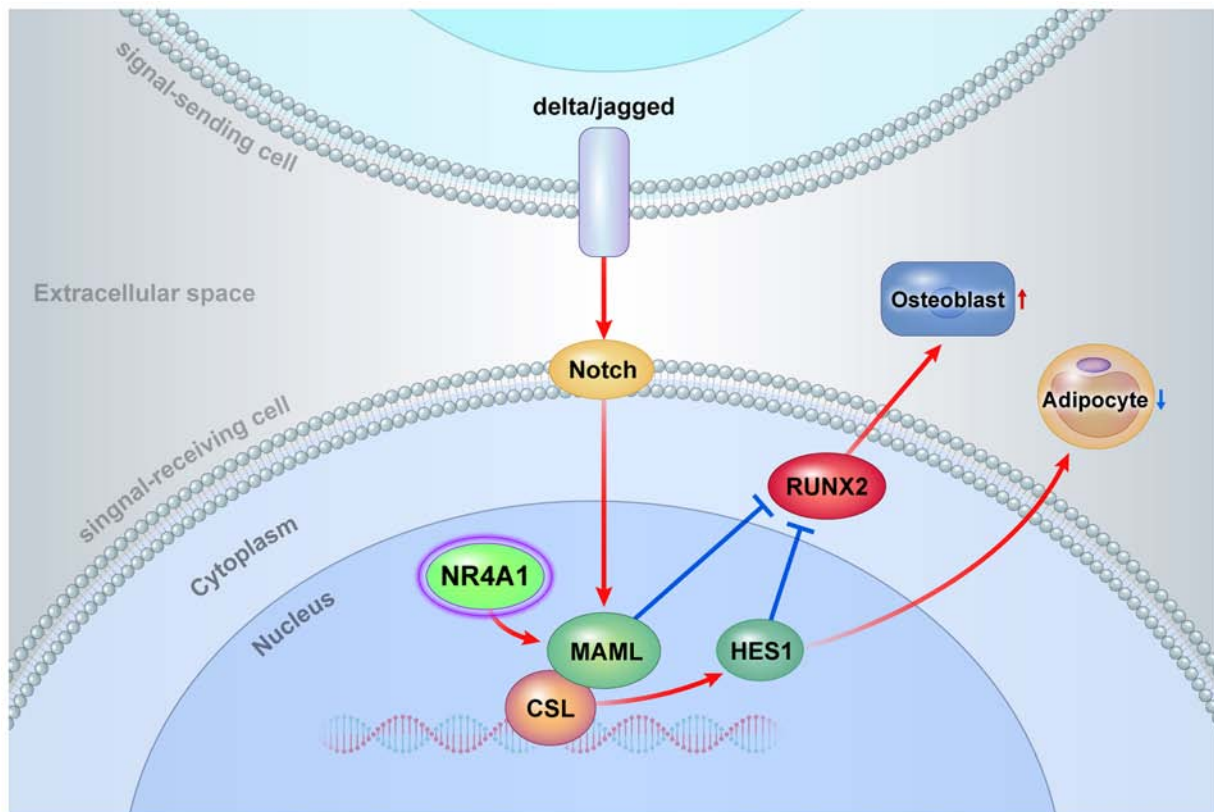


Figure 5. Mechanisms by which NR4A1 regulates osteoporosis and adipogenesis via the Notch signaling pathway. The reduction in NR4A1 expression led to a decrease in CSL-MAML-dependent Notch1 signaling, consequently triggering the upregulation of the RUNX2 gene, either via direct or indirect pathways involving HES1. This cascade promotes osteoblastogenesis. Moreover, the reduction of HES1 may further inhibit adipogenesis. NR4A1, nuclear receptor subfamily 4 group A member 1; RUNX2, Runt-related transcription factor 2; HES1, Hes family bHLH transcription factor 1.

signaling genes using real-time PCR revealed similar alterations in the expression of several genes, including *MAML3*, as shown by the IPA data. Various scientific investigations have established that the NR4A family exhibits interactive regulation of comparable target genes. For instance, Philips *et al* (43) and Carpentier *et al* (44) demonstrate that *NR4A1* and *NR4A2* (*Nurr1*) could potentially interact with adipogenic signaling pathways, such as Wnt pathways and glucocorticoid receptors. The expression of *NR4A1* and *NR4A3* is concomitantly reduced in cases of myelodysplastic syndromes (45). Hence, there is a plausible hypothesis that *NR4A1* may indirectly associate with the NOTCH pathway via *NR4A2* and *NR4A3*. Nevertheless, the present study suggested that altering expression of NR4A1 did not result in notable changes in the expression levels of *NR4A2* or *NR4A3*. Therefore, in human BMD-MSCs, NR4A1 may regulate osteoblastogenesis and adipogenesis via MAML3, a component of Notch signaling. The modulation of Notch signaling in mice, specifically targeting adipose tissue, leads to the induction of browning in white adipose tissue. This process promotes increased energy expenditure, enhances metabolic parameters and confers resistance to obesity (46). Brown adipose tissue (BAT) serves as an energy reservoir and plays a role in thermogenesis, leading to increased caloric expenditure (47). A notable upregulation of *NR4A1* in BAT has been reported (48). Hence, an association between NR4A1 and beige adipocytes is possible. However, the precise mechanisms underpinning the relationship between Notch and NR4A1 should be investigated in subsequent studies.

In the present study, the *Nr4a1* (*NR4A1*) overexpressing group showed more noticeable changes, especially in BMD-MSCs. However, an analysis of IPA showed that only a few genes had changes in expression linked to the Notch signaling pathway in the group that had increased NR4A1 levels, which could be attributed to several factors. Typically, a P-value ≤ 0.05 is used for DEG analysis, whereas in the present study, DEGs were evaluated using a stricter P-value threshold ($P < 0.01$), identifying a limited number of genes associated with the differences in gene expression patterns in cells undergoing genetic manipulation. This is evident from the identification of additional genes using a lenient P-value ≤ 0.05 (Fig. S6). The most represented processes, including canonical pathways, networks, upstream regulators, illnesses and biological functions, were listed by IPA following enrichment analysis. These findings suggested that it is essential to make subjective decisions about which data to use and how to integrate them for the required output (49). Even though the present study chose to focus on the Notch pathway, which encourages the formation of fat cells and hinders the formation of bone cells, the chance of another pathway, which was not thoroughly investigated, cannot be entirely dismissed. Therefore, further investigation is required.

In conclusion, NR4A1 has a negative role in osteoblastogenesis and a positive role in adipogenesis in MSCs. In addition, *Nr4a1* may affect the progression of osteoporosis and adipogenesis via the Notch signaling pathway (Fig. 5). Additional *in vivo* studies are needed to elucidate the role of NR4A1 in osteoblastogenesis and adipogenesis in MSCs.

Acknowledgements

Not applicable.

Funding

The present study was supported by grants from the National Research Foundation, Korea (grant nos. NRF-2019R1F1A1063188 and NRF-2022R1C1C1006818), and Ajou University Medical Center, Korea (grant no. 2023-C0460-00098).

Availability of data and materials

The data generated in the present study are included in the figures and/or tables of this article. The datasets generated or analyzed during the current study are available in the NCBI SRA database repository [BioProject: PRJNA941109; [https://www.ncbi.nlm.nih.gov/bioproject/?term=\(PRJNA941109\)%20AND%20bioproject_sra\[filter\]](https://www.ncbi.nlm.nih.gov/bioproject/?term=(PRJNA941109)%20AND%20bioproject_sra[filter])].

Authors' contributions

Conceptualization was by YJ, YS, IS, YSC and YJC. Methodology was by YJ, YS, and YJC. Validation was by YJ and YJC. Formal analysis was by YJ, YS and YJC. Investigation was by YJ. Data curation, original draft preparation and review and editing was by YJ. Reviewing and editing was by YJC. Visualization was by YJ. Supervision and project administration were by YJC. YJC and YJ confirm the authenticity of all the raw data. All authors read and approved the final manuscript.

Ethics approval and consent to participate

Not applicable.

Patient consent for publication

Not applicable.

Competing interests

The authors declare that they have no competing interests.

References

- Rosen CJ and Klibanski A: Bone, fat, and body composition: Evolving concepts in the pathogenesis of osteoporosis. *Am J Med* 122: 409-414, 2009.
- Kelly OJ, Gilman JC, Kim Y and Ilich JZ: Long-chain polyunsaturated fatty acids may mutually benefit both obesity and osteoporosis. *Nutr Res* 33: 521-533, 2013.
- Maurin AC, Chavassieux PM, Vericel E and Meunier PJ: Role of polyunsaturated fatty acids in the inhibitory effect of human adipocytes on osteoblastic proliferation. *Bone* 31: 260-266, 2002.
- Sheu Y, Amati F, Schwartz AV, Danielson ME, Li X, Boudreau R and Cauley JA; Osteoporotic Fractures in Men (MrOS) Research Group: Vertebral bone marrow fat, bone mineral density and diabetes: The Osteoporotic Fractures in Men (MrOS) study. *Bone* 97: 299-305, 2017.
- Scheller EL, Doucette CR, Learman BS, Cawthorn WP, Khandaker S, Schell B, Wu B, Ding SY, Bredella MA, Fazeli PK, *et al*: Region-specific variation in the properties of skeletal adipocytes reveals regulated and constitutive marrow adipose tissues. *Nat Commun* 6: 7808, 2015.
- Bredella MA, Fazeli PK, Miller KK, Misra M, Torriani M, Thomas BJ, Ghomi RH, Rosen CJ and Klibanski A: Increased bone marrow fat in anorexia nervosa. *J Clin Endocrinol Metab* 94: 2129-2136, 2009.
- Choi YJ, Song I, Jin Y, Jin HS, Ji HM, Jeong SY, Won YY and Chung YS: Transcriptional profiling of human femoral mesenchymal stem cells in osteoporosis and its association with adipogenesis. *Gene* 632: 7-15, 2017.
- Veum VL, Dankel SN, Gjerde J, Nielsen HJ, Solsvik MH, Haugen C, Christensen BJ, Hoang T, Fadnes DJ, Busch C, *et al*: The nuclear receptors NUR77, NURR1 and NOR1 in obesity and during fat loss. *Int J Obes (Lond)* 36: 1195-1202, 2012.
- Pearen MA and Muscat GE: Minireview: Nuclear hormone receptor 4A signaling: Implications for metabolic disease. *Mol Endocrinol* 24: 1891-1903, 2010.
- Zhao Y and Bruemmer D: NR4A orphan nuclear receptors: Transcriptional regulators of gene expression in metabolism and vascular biology. *Arterioscler Thromb Vasc Biol* 30: 1535-1541, 2010.
- Tetradis S, Bezouglaia O and Tsingotjidou A: Parathyroid hormone induces expression of the nuclear orphan receptor Nurrl in bone cells. *Endocrinology* 142: 663-670, 2001.
- Tetradis S, Bezouglaia O, Tsingotjidou A and Vila A: Regulation of the nuclear orphan receptor Nur77 in bone by parathyroid hormone. *Biochem Biophys Res Commun* 281: 913-916, 2001.
- Pirih FQ, Nervina JM, Pham L, Aghaloo T and Tetradis S: Parathyroid hormone induces the nuclear orphan receptor NOR-1 in osteoblasts. *Biochem Biophys Res Commun* 306: 144-150, 2003.
- Rajalin AM and Aarnisalo P: Cross-talk between NR4A orphan nuclear receptors and β -catenin signaling pathway in osteoblasts. *Arch Biochem Biophys* 509: 44-51, 2011.
- Lee SO, Abdelrahim M, Yoon K, Chintharlapalli S, Papineni S, Kim K, Wang H and Safe S: Inactivation of the orphan nuclear receptor TR3/Nur77 inhibits pancreatic cancer cell and tumor growth. *Cancer Res* 70: 6824-6836, 2010.
- Livak KJ and Schmittgen TD: Analysis of relative gene expression data using real-time quantitative PCR and the 2- $\Delta\Delta$ CT method. *Methods* 25: 402-408, 2001.
- Martin M: Cutadapt removes adapter sequences from high-throughput sequencing reads. *EMBnet J* 17: 10-12, 2011.
- Dobin A, Davis CA, Schlesinger F, Drenkow J, Zaleski C, Jha S, Batut P, Chaisson M and Gingeras TR: STAR: Ultrafast universal RNA-seq aligner. *Bioinformatics* 29: 15-21, 2013.
- Fu Y, Luo L, Luo N, Zhu X and Garvey WT: NR4A orphan nuclear receptors modulate insulin action and the glucose transport system: Potential role in insulin resistance. *J Biol Chem* 282: 31525-31533, 2007.
- Nagai S, Ikeda K, Horie-Inoue K, Takeda S and Inoue S: Estrogen signaling increases nuclear receptor subfamily 4 group A member 1 expression and energy production in skeletal muscle cells. *Endocr J* 65: 1209-1218, 2018.
- Qin DD, Yang YF, Pu ZQ, Liu D, Yu C, Gao P, Chen JC, Zong C, Zhang YC, Li X, *et al*: NR4A1 retards adipocyte differentiation or maturation via enhancing GATA2 and p53 expression. *J Cell Mol Med* 22: 4709-4720, 2018.
- Chao LC, Bensinger SJ, Villanueva CJ, Wroblewski K and Tontonoz P: Inhibition of adipocyte differentiation by Nur77, Nurrl, and Norl. *Mol Endocrinol* 22: 2596-2608, 2008.
- Martínez-González J, Rius J, Castelló A, Cases-Langhoff C and Badimon L: Neuron-derived orphan receptor-1 (NOR-1) modulates vascular smooth muscle cell proliferation. *Circ Res* 92: 96-103, 2003.
- Chong ZX, Yeap SK and Ho WY: Transfection types, methods and strategies: A technical review. *PeerJ* 9: e11165, 2021.
- Fumoto T, Yamaguchi T, Hirose F and Osumi T: Orphan nuclear receptor Nur77 accelerates the initial phase of adipocyte differentiation in 3T3-L1 cells by promoting mitotic clonal expansion. *J Biochem* 141: 181-192, 2007.
- Scholtyssek C, Ipseiz N, Böhm C, Krishnacoumar B, Stenzel M, Czerwinski T, Palumbo-Zerr K, Rothe T, Weidner D, Klej A, *et al*: NR4A1 regulates motility of osteoclast precursors and serves as target for the modulation of systemic bone turnover. *J Bone Miner Res* 33: 2035-2047, 2018.
- Pirih FQ, Aghaloo TL, Bezouglaia O, Nervina JM and Tetradis S: Parathyroid hormone induces the NR4A family of nuclear orphan receptors in vivo. *Biochem Biophys Res Commun* 332: 494-503, 2005.
- Lee SO, Andey T, Jin UH, Kim K, Singh M and Safe S: The nuclear receptor TR3 regulates mTORC1 signaling in lung cancer cells expressing wild-type p53. *Oncogene* 31: 3265-3276, 2012.

29. Lee SO, Li X, Hedrick E, Jin UH, Tjalkens RB, Backos DS, Li L, Zhang Y, Wu Q and Safe S: Diindolylmethane analogs bind NR4A1 and are NR4A1 antagonists in colon cancer cells. *Mol Endocrinol* 28: 1729-1739, 2014.
30. Hedrick E, Lee SO, Kim G, Abdelrahim M, Jin UH, Safe S and Abudayyeh A: Nuclear receptor 4A1 (NR4A1) as a drug target for renal cell adenocarcinoma. *PLoS One* 10: e0128308, 2015.
31. Hedrick E, Lee SO, Doddapaneni R, Singh M and Safe S: NR4A1 antagonists inhibit β 1-integrin-dependent breast cancer cell migration. *Mol Cell Biol* 36: 1383-1394, 2016.
32. Regan J and Long F: Notch signaling and bone remodeling. *Curr Osteoporos Rep* 11: 126-129, 2013.
33. Engin F, Yao Z, Yang T, Zhou G, Bertin T, Jiang MM, Chen Y, Wang L, Zheng H, Sutton RE, *et al*: Dimorphic effects of Notch signaling in bone homeostasis. *Nat Med* 14: 299-305, 2008.
34. Yorgan T, Vollersen N, Riedel C, Jeschke A, Peters S, Busse B, Amling M and Schinke T: Notch2 inactivation specifically in osteoblasts (Notch2^{fl/fl}/Runx2-Cre) leads to increased trabecular bone formation and enhanced osteogenic capacity, underscoring Notch2 as a key inhibitor of osteoblast differentiation. *Bone* 87: 136-146, 2016.
35. Dong Y, Jesse AM, Kohn A, Gunnell LM, Honjo T, Zuscik MJ, O'Keefe RJ and Hilton MJ: RBPjkappa-dependent Notch signaling regulates mesenchymal progenitor cell proliferation and differentiation during skeletal development. *Development* 137: 1461-1471, 2010.
36. Canalis E, Parker K, Feng JQ and Zanotti S: Osteoblast lineage-specific effects of notch activation in the skeleton. *Endocrinology* 154: 623-634, 2013.
37. Garcés C, Ruiz-Hidalgo MJ, Font de Mora JF, Park C, Miele L, Goldstein J, Bonvini E, Porrás A and Laborda J: Notch-1 controls the expression of fatty acid-activated transcription factors and is required for adipogenesis. *J Biol Chem* 272: 29729-29734, 1997.
38. Ross DA, Rao PK and Kadesch T: Dual roles for the Notch target gene Hes-1 in the differentiation of 3T3-L1 preadipocytes. *Mol Cell Biol* 24: 3505-3513, 2004.
39. Ugarte F, Ryser M, Thieme S, Fierro FA, Navratil K, Bornhäuser M and Brenner S: Notch signaling enhances osteogenic differentiation while inhibiting adipogenesis in primary human bone marrow stromal cells. *Exp Hematol* 37: 867-875.e1, 2009.
40. Wang X, Bledsoe KL, Graham RP, Asmann YW, Viswanatha DS, Lewis JE, Lewis JT, Chou MM, Yaszemski MJ, Jen J, *et al*: Recurrent PAX3-MAML3 fusion in biphenotypic sinonasal sarcoma. *Nat Genet* 46: 666-668, 2014.
41. Lin SE, Oyama T, Nagase T, Harigaya K and Kitagawa M: Identification of new human mastermind proteins defines a family that consists of positive regulators for notch signaling. *J Biol Chem* 277: 50612-50620, 2002.
42. Kannabiran C, Zeng X and Vales LD: The mammalian transcriptional repressor RBP (CBF1) regulates interleukin-6 gene expression. *Mol Cell Biol* 17: 1-9, 1997.
43. Phillips A, Maira M, Mullick A, Chamberland M, Lesage S, Hugo P and Drouin J: Antagonism between Nur77 and glucocorticoid receptor for control of transcription. *Mol Cell Biol* 17: 5952-5959, 1997.
44. Carpentier R, Sacchetti P, Ségard P, Staels B and Lefebvre P: The glucocorticoid receptor is a co-regulator of the orphan nuclear receptor Nurr1. *J Neurochem* 104: 777-789, 2008.
45. Mullican SE, Zhang S, Konopleva M, Ruvolo V, Andreeff M, Milbrandt J and Conneely OM: Abrogation of nuclear receptors Nr4a3 and Nr4a1 leads to development of acute myeloid leukemia. *Nat Med* 13: 730-735, 2007.
46. Bi P, Shan T, Liu W, Yue F, Yang X, Liang XR, Wang J, Li J, Carlesso N, Liu X, *et al*: Inhibition of Notch signaling promotes browning of white adipose tissue and ameliorates obesity. *Nat Med* 20: 911-918, 2014.
47. Gaspar RC, Pauli JR, Shulman GI and Muñoz VR: An update on brown adipose tissue biology: A discussion of recent findings. *Am J Physiol Endocrinol Metab* 320: E488-E495, 2021.
48. Hampton M, Melvin RG and Andrews MT: Transcriptomic analysis of brown adipose tissue across the physiological extremes of natural hibernation. *PLoS One* 8: e85157, 2013.
49. Cirillo E, Parnell LD and Evelo CT: A review of pathway-based analysis tools that visualize genetic variants. *Front Genet* 8: 174, 2017.



Copyright © 2024 Jin *et al*. This work is licensed under a Creative Commons Attribution-NonCommercial-NoDerivatives 4.0 International (CC BY-NC-ND 4.0) License.